ELSEVIER

Contents lists available at ScienceDirect

Earth and Planetary Science Letters

journal homepage: www.elsevier.com/locate/epsl



Tectonic modulation of caldera volcanism on the South Aegean Volcanic Arc

Abigail Metcalfe ^{a,*}, Tim Druitt ^a, Katharina Pank ^b, Steffen Kutterolf ^b, Jonas Preine ^{c,d}, Sarah Beethe ^e, Axel Schmitt ^f, Christian Hübscher ^c, Paraskevi Nomikou ^g, Thomas A. Ronge ^h, Carole Berthod ⁱ, Hehe Chen ^j, Shun Chiyonobu ^k, Acacia Clark ^l, Susan DeBari ^m, Ralf Gertisser ⁿ, Raymond Johnston ^o, Olga Koukousioura ^p, Michael Manga ^q, Molly McCanta ^r, Iona McIntosh ^s, Ally Peccia ^t, Masako Tominaga ^d, Yuzuru Yamamoto ^u, Adam Woodhouse ^v, Alexis Bernard ^w, Tatiana Fernandez Perez ^x, Christopher K. Jones ^y, Kumar Batuk Joshi ^z, Günther Kletetschka ^{aa}, Antony Morris ^{bb}, Paraskevi Polymenakou ^{cc}, Xiaohui Li ^{dd}, Dimitrios Papanikolaou ^g, David Pyle ^{ee}, Pietro Sternai ^{ff}

^a University Clermont-Auvergne, CNRS, IRD, OPGC, Laboratoire Magmas et Volcans, Clermont-Ferrand, France

^b GEOMAR Helmholtz Centre for Ocean Research Kiel, Wischhofstrasse 1-3, D-24148 Kiel, Germany

^c Institute of Geophysics, University of Hamburg, Bundesstrasse 55, D-20146 Hamburg, Germany

^d Department of Geology and Geophysics, Woods Hole Oceanographic Institution, Woods Hole MA 02543, USA

^e College of Earth, Ocean, and Atmospheric Sciences, Oregon State University, Corvallis OR 97333, USA

f John de Laeter Centre, Curtin University, 6845 Bentley, Australia

g Department of Geology and Geoenvironment, National and Kapodistrian University of Athens, 15784 Athens, Greece

h Texas A&M University, College Station TX 77845, USA

ⁱ Institut De Physique Du Globe De Paris, Centre National de la Recherche Scientifique (CNRS), 75005 Paris, France

^j School of Ocean Sciences, China University of Geosciences, 100083 Haidan District, Beijing, China

k Faculty of International Resource Sciences, Akita University, Akita, Akita Prefecture 0108502, Japan

¹ School of Natural Sciences/CODES, University of Tasmania, Hobart 7005, Australia

^m Geology Department, Western Washington University, Bellingham WA 98225, USA

 $^{^{\}rm n}$ School of Life Sciences, Keele University, Keele, Staffordshire ST5 5BG, UK

[°] School of Geosciences, University of South Florida, Tampa FL 33620, USA

^p School of Geology, Aristotle University of Thessaloniki, 54124 Thessaloniki, Greece

^q Department of Earth and Planetary Science, University of California, Berkeley, CA 94720, USA

r Department of Earth and Planetary Sciences, University of Tennessee, Knoxville TN 37996-1526, USA

s Japan Agency for Marine-Earth Science and Technology, 2-15 Natsushima-cho, Yokosuka Kanagawa 237-0061, Japan

^t Lamont-Doherty Earth Observatory, Columbia University, Palisades NY 10964, USA

^u Graduate School of Science, Kobe University, 1-1 Rokkodai-cho, Nada-ku, Kobe, Hyogo 657-8501, Japan

^v School of Earth and Environmental Sciences, Cardiff University, Cardiff, CF10 3AT, UK

w Laboratoire des Fluides Complexes et leurs Réservoirs, Université de Pau et des Pays de l'Adour, F-64000 Pau, France

x Department of Geology, Kent State University, 221 McGilvrey Hall, 325 S Lincoln Street, Kent OH 44242, USA

y Department of Earth and Planetary Sciences, University of California, Riverside CA 92506, USA

² Department of Geology, Central University of Himachal Pradesh, Dharamshala, Kangra, 176206, India

^{aa} Geophysical Institute, University of Alaska Fairbanks, 2156 Koyukuk Drive, Fairbanks AK 99775, USA

bb School of Geography, Earth and Environmental Sciences, Plymouth University, Drake Circus, Plymouth PL4 8AA, UK

cc Institute of Marine Biology, Biotechnology and Aquaculture, Hellenic Centre for Marine Research, Heraklion, Greece

dd Key Laboratory of Submarine Geoscience and Prospecting Techniques, Ocean University of China, Qingdao, China

ee Department of Earth Sciences, University of Oxford, South Parks Road, Oxford, OX1 3AN, UK

ff Department of Earth and Environmental Sciences, University of Milano-Bicocca, Milan, Italy

^{*} Corresponding author.

E-mail address: abigail.metcalfe@uca.fr (A. Metcalfe).

ARTICLE INFO

Editor: Dr C. M. Petrone

Keywords: Caldera Tectonic modulation Megabed Explosive eruption Thermal runaway Ignimbrite flare-up

ABSTRACT

Many highly hazardous, caldera-forming explosive eruptions occur in extensional tectonic regimes, but the role of lithospheric rifting in modulating caldera volcanism remains enigmatic. IODP Expedition 398 deep-drilled the volcano-sedimentary infills of submarine half-grabens around Santorini caldera on the continental South Aegean Volcanic Arc. Here we use the volcanic tephra archives to produce a high-resolution eruptive chronostratigraphy for Santorini, to ground-truth seismic stratigraphy, and to extract an integrated timeline of volcano-tectonic couplings. The rift basins contain several submarine volcaniclastic megabeds from the caldera-forming eruptions of Santorini and one from the Kos caldera. The thickest megabed succession is < 250,000 yrs old and lies on a seismic reflection onlap surface that records a phase of rapid rifting. Sedimentation lagged behind subsidence during this rifting phase, creating bathymetric troughs. Integrating submarine core-seismic and onland datasets, we propose that rifting may have driven the transition of Santorini from a prolonged state of effusive and minor explosive activity (~550 - 250 ka) typical of arc stratovolcanoes to one of repeated caldera-forming eruptions (<250 ka). Rapid rifting may have amplified the normal internal dynamics of the magmatic system in three ways, driving the volcano into a sustained, highly explosive state: (1) an increase in the supply of mantle-derived basalt, (2) enhanced shearing, permeability, and melt percolation in the transcrustal magmatic system, and (3) the development of horizontally extensive magma reservoirs. Broadly simultaneous transitions into calderaforming activity of the widely separated Santorini and Kos Volcanoes suggest that the two magmatic systems are linked by plate-scale lithospheric stresses.

1. Introduction

Caldera-forming explosive eruptions of volcanoes discharge large volumes of silicic magma and impact humans, infrastructures and environments on local to global scales (Newhall et al., 2018; Cassidy and Mani, 2022). Several decades of research have led to models of the internal controls of caldera volcanism. The mantle-derived basalt that drives caldera systems generates silicic magmas by fractional crystallisation, crustal melting, and pluton defrosting in transcrustal mush systems (Bachmann and Huber, 2016; Cashman et al., 2017; Sparks et al., 2019). Caldera-forming eruptions occur when the fluxes of melts, fluids and heat into the crust are sufficiently high to raise the brittle-ductile transition and create the crustal rheological conditions necessary for the growth and maturation of large magma reservoirs (Jellinek and DePaolo, 2003; Degruyter et al., 2016; Townsend et al., 2019). These reservoirs can then trap the ascending melts in a thermomechanical runaway, leading to caldera-forming eruptions (Karakas and Dufek, 2015; Bouvet de Maisonneuve et al., 2021).

However, the internal processes of sub-caldera magmatic systems can be influenced by lithospheric tectonics (here used to describe the upper plate strain in a subduction-driven system; Fig. S1). This is particularly true in extensional environments such as continental rift zones (e.g., East African Rift, Hutchison et al., 2016; Taupō Volcanic Zone, Wilson et al., 2009; South Aegean Volcanic Arc, Hooft et al., 2017). Many calderas lie in extensional settings, suggesting that rifting helps promote mantle inputs high enough to push the magmatic systems over the threshold into the caldera-forming state (Hughes and Mahood, 2008; Burns et al., 2015). However, tectonic strain and internal magmatic processes at caldera systems operate on variable timescales, from 10^0 yr for eruption triggering to 10^6 – 10^7 yr for large ignimbrite flare-ups, making it challenging to establish causal relationships (Gravley et al., 2016; Sternai, 2020; Berryman et al., 2022; Muirhead et al., 2022; Brune et al., 2023). While the effects of lithospheric extension on the locations of rift-hosted volcanoes, and the feedbacks between magmatism and crustal stresses, have been widely investigated (Rowland et al., 2010; Brune et al., 2023), the effects of rifting on volcanic eruption style and magnitude at caldera systems are, with some exceptions (Wilson et al., 2009; Gravley et al., 2016; Hutchison et al., 2016), less well understood.

Here we investigate the inter-relationships between lithospheric rifting and caldera volcanism at Santorini Volcano (South Aegean Volcanic Arc; Fig. 1a) on the 10^4 – 10^5 yr timescales characteristic of arc volcano caldera cycles. The volcanic history of Santorini has been partly unraveled by studies of marine tephrostratigraphy and on-island volcanic products (Fig. 1b; Druitt et al., 1999; Wulf et al., 2020; Kutterolf

et al., 2021), and the offshore seismic stratigraphy of the surrounding rift basins has been documented and interpreted (Hübscher et al., 2015; Nomikou et al., 2016, 2018; Tsampouraki-Kraounaki et al., 2021; Preine et al., 2022a,b). A close relationship between faults, dyke swarms, and volcanic vents with structural lineaments at and around Santorini has been shown to reflect a crustal tectonic influence (Kokkalas and Aydin, 2012; Feuillet, 2013; Hooft et al., 2017; Tsampouraki-Kraounaki et al., 2021; Preine et al., 2022a,b; Drymoni et al., 2022), and analysis of the distribution and orientation of faults and fractures from seismic tomography data suggests a fundamental influence of regional-scale stresses (Heath et al., 2021). Preine et al. (2022a) proposed from interpretation of seismic stratigraphy that a period of caldera-forming explosive volcanism on Santorini was preceded by a phase of rapid rift extension. Testing this hypothesis requires well-dated, high-resolution records of both volcanic and tectonic events that can be precisely correlated. IODP (International Ocean Discovery Program) Expedition 398 deep-drilled the volcano-sedimentary infills of marine rift basins around Santorini (Druitt et al., 2024b). Explosive eruptions shower ash and/or pour pyroclastic currents into the marine basins, generating a rich archive of volcanic events that is potentially more complete, and extends further back in time, than that recorded onland (Fig. 2). Using biostratigraphic and tephrostratigraphic age constraints, and integrating the published seismic stratigraphy, we investigate a volcano-tectonic link at Santorini and discuss possible mechanisms of couplings and feedbacks between lithospheric extension and caldera volcanism on the South Aegean Volcanic Arc.

2. The volcano-tectonic setting

The volcanoes of Santorini and the adjacent submarine Kolumbo volcanic chain (Kolumbo seamount and >20 smaller eruptive centres) lie on \sim 25 km of stretched continental crust (Hooft et al., 2017) (Fig. 1a). Along with the extinct Christiana Volcano, they form the Christiana-Santorini-Kolumbo Volcanic Field, one of five volcanic fields on the South Aegean Volcanic Arc (Vougioukalakis et al., 2019). Christiana was active in the Pliocene through to the Early Pleistocene, but has been extinct since \sim 1.6 Ma (Preine et al., 2022b). Santorini has had two main phases of development (Fig. 1b):

Ancient Santorini (>550 ka), also known as 'old' or 'ancestral'
 Santorini, erupted calcalkaline rhyolites from shallow-submarine to
 subaerial vents between >650 and 550 ka (the onland 'Early Centres
 of Akrotiri' of Druitt et al., 1999). Druitt et al. (2024a) also identified
 a voluminous (Dense Rock Equivalent volume >30 km³) submarine
 rhyolitic pumice deposit, the Archaeos Tuff, from a mid-Pleistocene

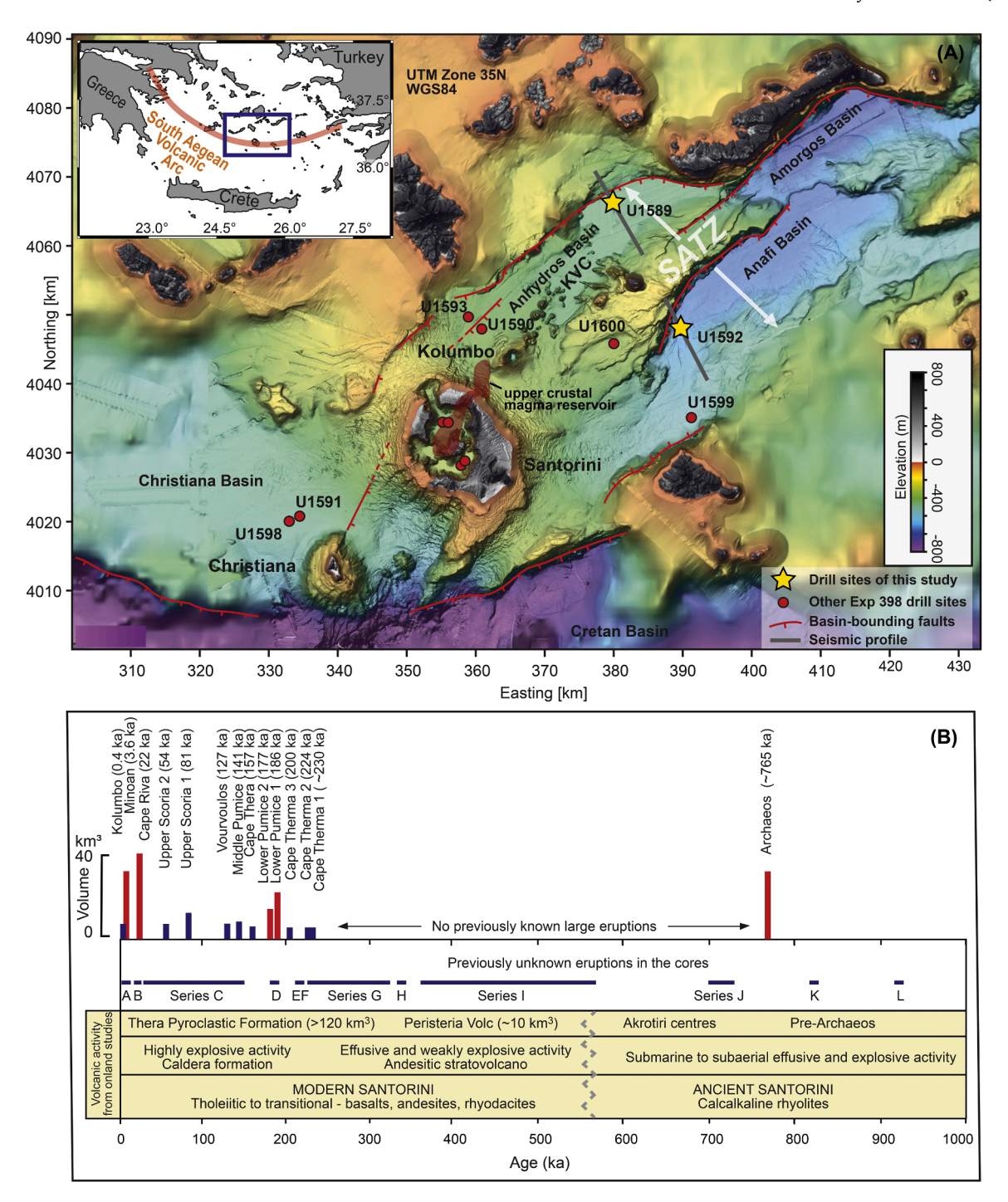


Fig. 1. (a) Location of the Christiana-Santorini-Kolumbo Volcanic Field and its relationship to the Santorini-Amorgos Tectonic Zone (SATZ) on the South Aegean Volcanic Arc (inset: blue rectangle) and of the IODP drilling sites outside of Santorini caldera (red dots, with site numbers). The two sites most relevant to the present paper (U1589 and U1592) are shown as yellow stars. Basin-bounding faults are shown in red, with ticks on the down-thrown side. The semi-transparent brown areas marks the upper crustal storage zone imaged by McVey et al. (2019). KVC: Kolumbo Volcanic Chain. See Methods for sources of bathymetric data. Modified from Druitt et al., (2024a). (b) Summary of the explosive volcanic history of Santorini Volcano, showing the main eruptions that produced the volcanic layers found in the IODP cores. The named eruptions known previously from onland studies (Druitt et al., 1999) are shown as vertical bars, the heights of which are proportional to eruptive volume (dense-rock equivalent (Kutterolf et al., 2021; Druitt et al., 2024a). Large caldera-forming silicic eruptions (CFSE in the main text) are shown as red bars, and smaller explosive eruptions as blue bars. Eruptions relating to previously unknown volcanic layers discovered in the IODP cores of the present paper are shown as blue horizontal lines and labelled by a letter corresponding to the name given either to a given tephra layer or to a series of tephra layers. The yellow boxes show the corresponding timeline of volcanic activity known previously from onland studies.

explosive eruption of Ancient Santorini in cores from IODP Expedition 398. The age of the Archaeos eruption was estimated as 520 ka using biostratigraphic data, but $^{40}\mathrm{Ar}/^{39}\mathrm{Ar}$ plagioclase and U-Pb zircon dating now place it at $\sim\!765$ ka (S. Beethe and A.K. Schmitt, unpublished data).

• Modern Santorini (<550 ka) has erupted basalts to rhyodacites that are tholeiitic to transitional tholeiitic-calcalkaline in character. Its history can be divided into two broad stages. For the first $\sim\!300$ kyr, Modern Santorini exhibited the effusive and weakly explosive behavior typical of andesitic stratovolcanoes (including the $<\!10$

km³, 530 – 430 ka 'Peristeria' stratocone; Druitt et al., 1999). It then transitioned at ~250 ka into a series of highly explosive explosions that discharged >120 km³ of intermediate to silicic magma and laid down the 'Thera Pyroclastic Formation' (TPF) (Druitt et al., 1999; Kutterolf et al., 2021). At least four of the TPF eruptions formed calderas, grouped into two time packages: 186 – 177 ka (Lower

Pumice 1 and Lower Pumice 2) and 22 – 3.6 ka (Cape Riva and Minoan). The TPF stage of Modern Santorini is characterized by (1) a concentration of highly explosive activity, (2) repeated Caldera-Forming Silicic Eruptions (CFSEs), and (3) a high volcanic output (Fig. 1b).

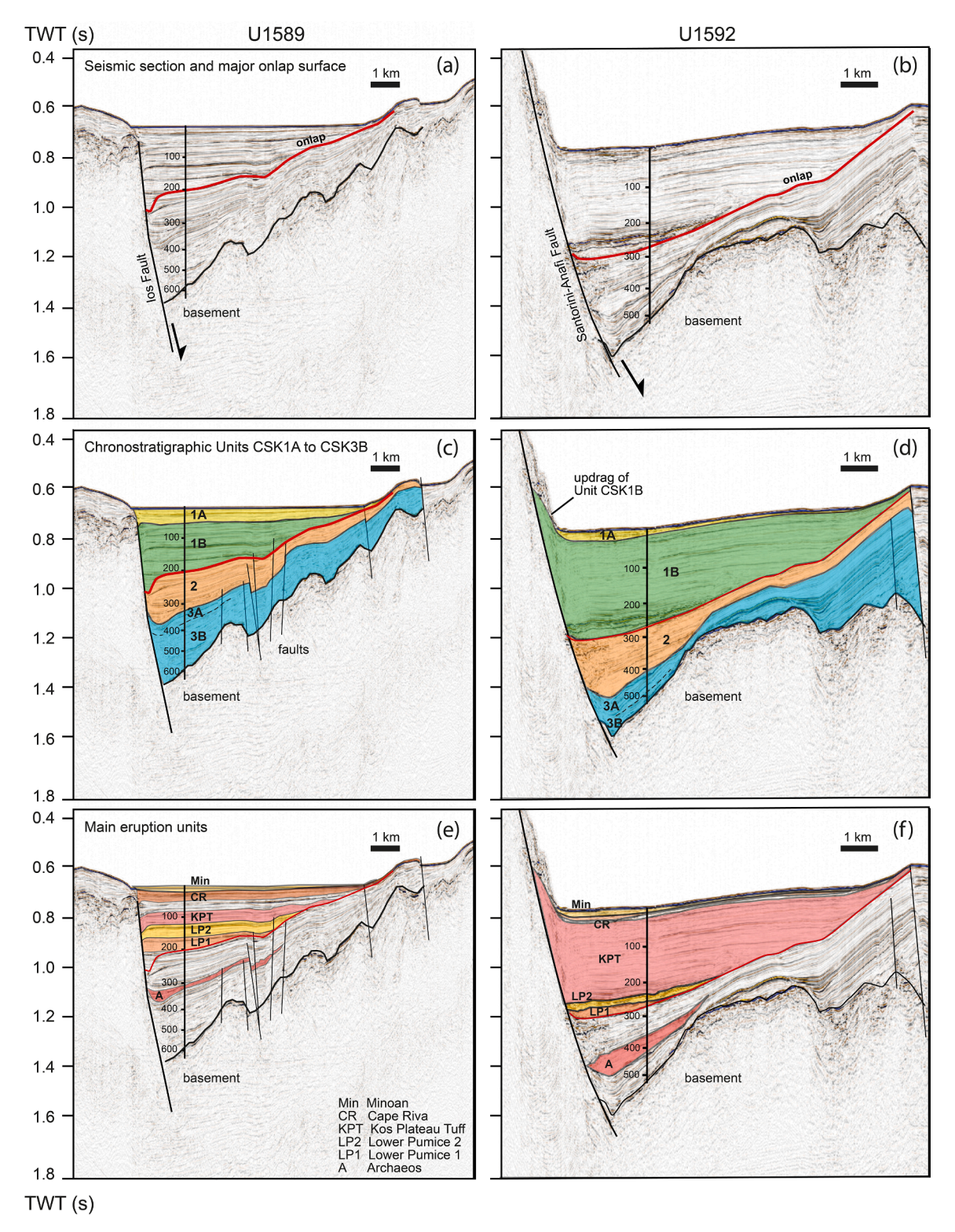


Fig. 2. (a-b) Seismic profiles for the Anhydros and Anafi basins with the major onlap surface shown in red. (c-d) Chronostratigraphic units, described in the text. (e-f) The caldera-forming silicic eruptions (CFSE in the main text) of Santorini and the Kos Plateau Tuff from the Kos Volcano. Core-seismic integration from Preine et al. (2025).

Kolumbo Volcano last erupted explosively in 1650 CE, and seismic profiles across it reveal multiple, stacked edifices from older eruptions (Hübscher et al., 2015).

Santorini lies at the southern end of a NE-SW system of en-echelon continental rift basins (Santorini-Amorgos Tectonic Zone; SATZ) that cut the volcanic arc and extend into the back-arc region (Nomikou et al., 2016, 2018; Hooft et al., 2017; Tsampouraki-Kraounaki et al., 2021). Extension of the SATZ is driven by slab rollback and lateral bending, facilitated by slab tears underneath the Anatolian plate and eastern Aegean (Jolivet et al., 2013; Sternai et al., 2014). The possible existence of a right-lateral oblique component to the faulting is debated (Tsampouraki-Kraounaki et al., 2021; Crutchley et al., 2023). Three half-graben basins (Anhydros, Anafi, Amorgos) defined by multiple overstepping normal faults and relay ramps constitute the SATZ (Hooft et al., 2017; Crutchley et al., 2023) (Figs. 1a and 2). While the western Anhydros Basin contains the Kolumbo Chain volcanoes, the Anafi Basin and eastern Anhydros Basin are non-volcanic (Hübscher et al., 2015; Nomikou et al., 2016; Preine et al., 2022a), Seismic tomography has imaged a NE-SW elongated upper-crustal reservoir of melt-bearing magmatic crystal mush that extends from Santorini towards Kolumbo (Fig. 1a; McVey et al., 2019). Other melt storage regions have been imaged seismically NE of Santorini at mid-crustal depths (Autumn et al., 2025; Hufstetler et al., 2025).

A dense array of single and multichannel seismic profiles across the SATZ reveals rift sediment fills up to 1.4 km thick, with multiple seismic stratigraphic packages (Hübscher et al., 2015; Nomikou et al., 2016, 2018; Preine et al., 2022a, b). The SATZ is cut to the south by the earlier, ENE-WSW Christiana Basin of Pliocene age (Heath et al., 2019; Preine

et al., 2022b) (Fig. 1a).

3. Materials and methods

IODP Expedition 398 deep-drilled eight sites outside of Santorini caldera on the R/V JOIDES Resolution (Fig. 1a). We here focus on Site U1589 in the Anhydros Basin and Site U1592 in the Anafi Basin, each of which hosts a different sediment distributary branch of the volcanic field. The drill cores were logged on board (Fig. 3; Table S1), taking into account artefacts of drilling and core recovery such as sediment mixing, shear-induced uparching, brecciation, biscuiting and ash liquefaction (Jutzler et al. 2025). Physical properties including sediment density and P-wave velocity were measured in situ on the cores. Samples of the volcanic layers were collected for chemical analysis of glass shards for chemical fingerprinting and correlation purposes: major elements by electron microprobe and trace elements by laser-ablation ICPMS (Table S2). Correlations used previously published databases of glass chemistry from studies of Santorini and Kolumbo tephras in shallow gravity cores (Kutterolf et al., 2021). Descriptions of volcanic layers from previously known eruptions (Table S3) are given in Table S4, and those of the newly recognized eruptions are given in Table S5. Ages of some volcanic layers were determined by chemical correlation with marine tephra layers from published studies of shallow marine gravity cores, the ages of which are already known (Table S3; Wulf et al., 2020; Kutterolf et al., 2021). Biostratigraphic ages of the sediments were determined shipboard using assemblages of foraminifera and calcareous nannofossils, based on one sample per 9.5 m or 4.7 m core (Tables S6 and S7). Sapropels of previously known age were recognized using the criteria of

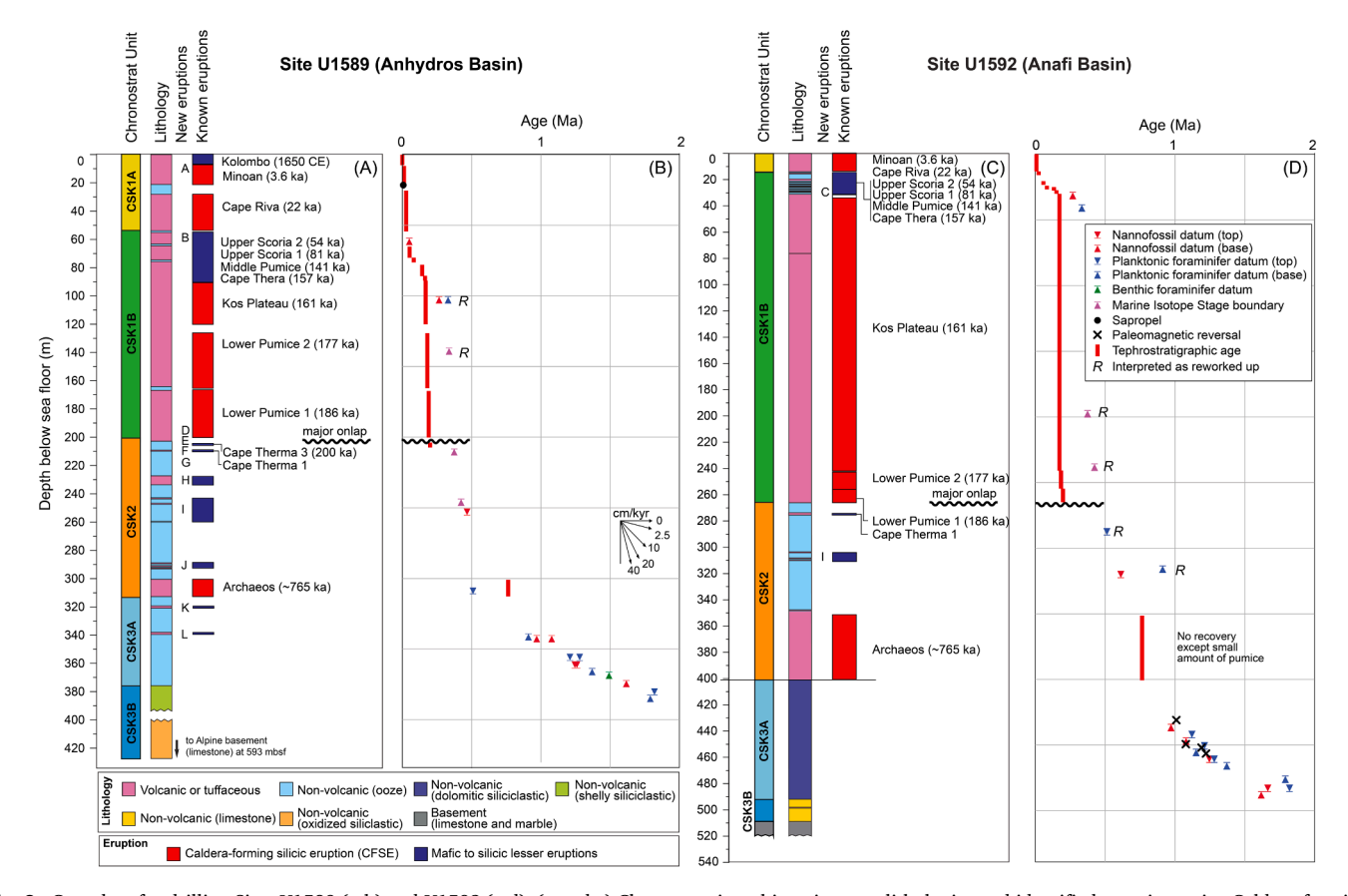


Fig. 3. Core data for drilling Sites U1589 (a-b) and U1592 (c-d). (a and c) Chronostratigraphic units, core lithologies and identified eruption units. Caldera-forming silicic eruptions are shown in red, and smaller eruptions in blue. The letters denote the newly recognized tephra A to L. (b and d) Age-depth curves based on biostratigraphic and tephrostratigraphic constraints. The red bars are previously known volcanic layers of known ages (Wulf et al., 2020; Druitt et al., 2024a). The biostratigraphic ages are taken from Druitt et al. (2024b); those <0.5 Ma are commonly older than tephrostratigraphic ages due to upward reworking associated with the very high sedimentation rates. Biostratigraphic ages >0.5 Ma are considered to be reliable as the associated sedimentation rates were lower. Magnetic reversal data are taken from Druitt et al. (2024b) and are in broad agreement with the biostratigraphic ages.

Rohling et al. (2015). Ages of previously unknown eruptions were estimated by extrapolating sedimentation rates between horizons of known age (Table S8). These age estimates are approximate due to the highly dynamic sedimentary environments of the rift axes, and they will be refined in a future publication integrating data from all the drill sites. The core chronostratigraphy was integrated with previously published seismic stratigraphy to create an integrated record of volcanism and tectonics (Fig. 2; Preine et al., 2025). See the Supplementary Text for full details of the methods used.

4. Results

4.1. Rift basin stratigraphy

Drilling penetrated the entire rift volcano-sedimentary fills and bottomed out in limestone/marble basement at both sites (593 mbsf [meters below sea floor] at U1589 and 510 mbsf at U1592; Figs. 2 and 3). The drilling recoveries above basement were 78 % (Hole A) and 92 % (Hole B) at Site U1589, and 71 % (Hole A) and 50 % (Hole B) at Site U1592 (Fig. S2). We divide the rift fills into five chronostratigraphic Units, CSK1A, CSK1B, CSK2, CSK3A and CSK3B from the top down, based on biostratigraphic, tephrostratigraphic, and seismic-stratigraphic data (Fig. 3; Tables 1 and S9). Unit CSK1A is dominated by lapilli ashes of silicic composition. Units CSK1B and CSK2 have upper parts dominated by oozes with many thin ashes of mafic to silicic composition and lower parts dominated by thick silicic lapilli ashes. Unit CSK3A consists of oozes and sands (dolomitic at Site U1592) with dispersed ash layers, and Unit CSK3B consists of siliciclastic sediments and bioclastic limestones. The basement at each site comprises limestones or marbles of Early Pleistocene to Cretaceous age.

The volcanic layers present in Units CSK1A to CSK3A range from beds <0.1 m thick to megabeds several tens (and in one case more than two hundred) of meters thick (Fig. 2; Figs. S3 to S7). By 'megabed' we mean an unusually thick and laterally extensive bed that differs in

composition from the host sediments (e.g., Sawyer et al., 2023; Druitt et al., 2024a). We attribute most of the volcanic layers to eruptions based on an abundance of glassy ash and lapilli, and to the chemical uniformity of vitric components (Figs. 4 and S8), while recognizing reworked volcanic layers by the presence of multiple vitric populations or abundant lithics.

The products of most Santorini explosive eruptions known from onland studies (Fig. 1b) are recognized in the cores, based on chemical correlations (Tables 1 and S4; Figs. 2-4; Fig. S8). The Minoan (3.6 ka) and Cape Riva (22 ka) eruptions occur in chronostratigraphic Unit CSK1A, the Upper Scoria 2 (54 ka) to Lower Pumice 1 (186 ka) eruptions occur in Unit CSK1B, and the Cape Therma 1 (230 \pm 10 ka) to Archaeos (~765 ka) eruptions occur in Unit CSK2. Tephra from three of the eruptions occur within sapropels (Upper Scoria 1 in Sapropel S3 at Site U1592; Lower Pumice 2 in Sapropel S6 and Cape Therma 3 in Sapropel S7 at Site U1589), as previously noted (Wulf et al. 2020). Biotite-bearing rhyolitic pumice from the 1650 CE eruption of Kolumbo Volcano occurs at the top of Unit CSK1A, and is the youngest volcanic layer in the cores. In both basins an extensive megabed of graded ash (up to 210 m at Site U1592) is present in Unit CSK1B between the Lower Pumice 2 (177 ka) and Cape Thera (157 ka) eruptions. This unit correlates chemically and mineralogically with the Kos Plateau Tuff (161 ka) from Kos caldera, 120 - 140 km to the east (Metcalfe et al., 2025). We show the four CFSEs of Modern Santorini, the Archaeos Tuff of Ancient Santorini, and the Kos Plateau Tuff in warm colors on Fig. 2e and f.

Forty previously undocumented tephra layers occur in the cores (Fig. 3; Tables 1 and S5), some of which we grouped into stratigraphically and compositionally related tephra series (Fig. 4). Tephra A is a biotite-bearing rhyolitic ash that has a trace element chemistry similar to that of the 1650 CE eruption of Kolumbo. Tephras B to H have the chemistries of magmas from Modern Santorini, with the exception of B and E, which derive from unknown sources, possibly Kolumbo. Tephra Series I is andesitic to dacitic; most of the ash layers compositionally overlap the fields for the onland Peristeria center (Modern Santorini),

Table 1Summary of rift volcanic stratigraphy.

Chronostratigraphic Unit	Depth U1589 mbsf	Depth U1592 mbsf	Composition	Age (ka)	Eruptions and ages*
CSK1A	0 – 53	0 – 15	Silicic lapilli ashes	0.4 – 26	Kolumbo, 0.4 ka <i>Tephra A, 1.5 ka</i> Minoan, 3.6 ka
	53 – 86	15 – 31	Oozes with multiple ashes	54 – 157	Cape Riva, 22 ka <i>Tephra B, 24 ka</i> Upper Scoria 2, 54 ka
CSKID	33 – 60	15 – 31	Oozes with multiple asiles	34 – 137	Upper Scoria 1, 81 ka Middle Pumice, 141 ka
	86 – 200	31 – 266	Silicic lapilli ashes	161 – 186	<i>Tephra series C, 26 - 150 ka</i> Cape Thera, 157 ka Kos Plateau, 161 ka
		01 200	omete aipini doneo	100	Lower Pumice 2, 177 ka Lower Pumice 1, 186 ka
CSK2	200 - 302	266 – 348	Oozes with multiple ashes	200 – 725	Tephra D, 189 ka Cape Therma 3, 200 ka Tephra E, 209 ka Tephra F, 210 ka Cape Therma 1, 230 \pm 10 ka Tephra Series G, 221- 326 ka Tephra H, 337 ka
					Tephra series I, 359 - 577 ka Tephra series J, 699 - 726 ka
CSK3A	302 - 313 313 - 375	348 - 402 402 - 490	Silicic lapilli ash Oozes with rare ashes (U1589)	~765 ~765 – 1600	Archaeos, ~765 ka Tephra K, 821 ka Tephra L, 918 ka
CSK3B	375 – 593	490 – 510	Siliciclasts (U1592) Siliciclastics (U1589)	1600 – 2000	
Basement	>593	>510	Bioclastic limestone (U1592) Limestone and marble	Eocene to Cretaceous (U1589) Early Pleistocene (U1592)	

^{*} Age estimates of previously unknown (lettered) tephras or tephra series are approximate

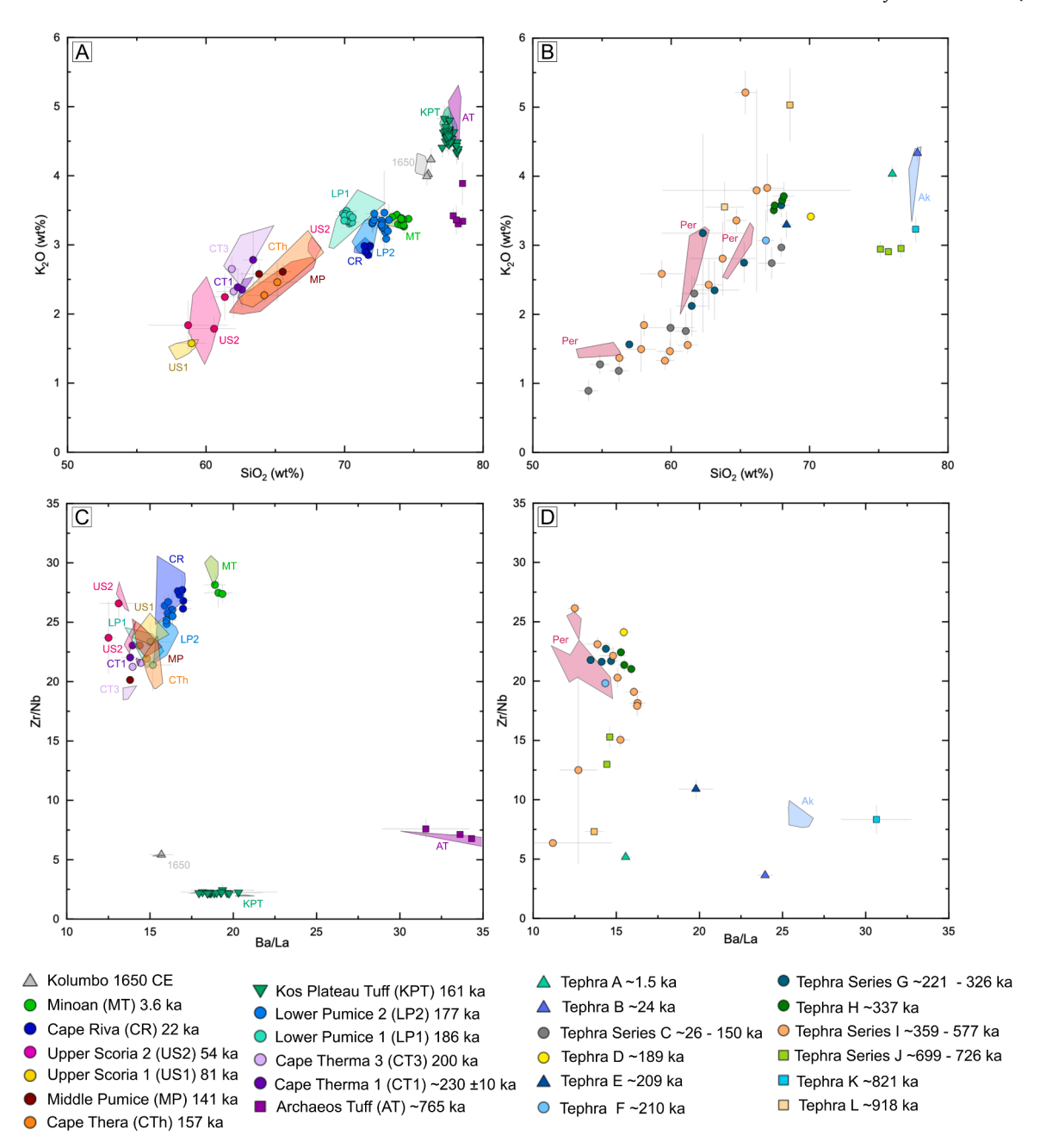


Fig. 4. Major and trace element discrimination diagrams for volcanic layers in the cores of Sites U1589 and U1592. (a and c) Glass compositions from the cores (data points) that correlate with previously known eruptions (colored fields showing the compositional ranges from previous studies, Kutterolf et al., 2021; Druitt et al., 2024a). Also shown are the known compositional ranges for Peristeria (Per) and Akrotiri (Ak) onland volcanics (new glass analyses in table S2). (b and d) Glass compositions from the cores for previously unknown eruptions or series of eruptions (Tephra layers or Tephra series A to L, with the data points for series enclosed by colored fields.

while some with higher K_2O and lower Zr/Nb may derive from other, as yet undetermined, volcanic fields. Tephra Series J is rhyolitic with a chemical signature intermediate between Modern and Ancient Santorini, while Tephra K, also rhyolitic, chemically resembles the Archaeos Tuff. Tephra L is high in K_2O , and may derive from a different volcanic field. With the exception of Tephra H (>4 m thick), all these layers are \leq 42 cm thick, and are volumetrically much smaller than the TPF megabeds.

4.2. Age-depth relationships

The age-depth curves obtained by integrating biostratigraphic ages with tephrostratigraphic ages for the previously dated volcanic units

reveal that the tephrostratigraphic ages are generally younger than the biostratigraphic ages in Units CSK1A, CSK1B and CSK2 (Fig. 3). We attribute this to upward reworking of microfossils in the highly dynamic rift environments. In what follows we use the tephrostratigraphic ages in Units CSK1A, CSK1B and CSK2 and the biostratigraphic ages in Unit CSK3A (no ages were obtained from Unit CSK3B). Estimated ages of Tephras A to L are given in Table 1. The base of Unit CSK3A has an age of $\sim\!1.6$ Ma; by extrapolation, we estimate that the base of Unit CSK3B at Site U1592 would be $\sim\!2$ Ma and at Site U1589 (where CSK3B is thicker) would be $>\!2$ Ma (Fig. 3). Biostratigraphic dating of cores from Site U1599 (Fig. 1a) provides an even earlier constraint on the onset of rifting of the Anafi Basin ($>\!2.7$ Ma; Druitt et al. 2024b).

4.3. Core-seismic correlation

Correlation of the core chronostratigraphy with the published seismic stratigraphy reveals a consistent seismo-stratigraphy of the Anhydros and Anafi Basins (Fig. 2). Preine et al. (2022a,b) recognized six seismic stratigraphic packages in each of the two basins. They also recognized two major seismic reflection onlap surfaces: one (their onlap surface h4) that is particularly prominent in the Anhydros Basin and the other (their onlap surface h6) that is prominent in the Anafi Basin. They interpreted these onlaps as recording phases of rapid subsidence with relatively little sedimentation ('rift pulses'). The IODP Exp. 398 cores now make it possible to redefine the previously only visual correlation between the two basins (Table S9), such that the two major onlap surfaces previously identified are in fact the same (shown as a solid red line on Fig. 2a-b). This single major onlap surface directly underlies Unit CSK1B; it is formed of inclined packages of marine sediments and minor tephra layers of Unit CSK2, and is directly overlain by thick packages of CFSE megabeds of the TPF and Kos Plateau Tuff eruptions.

4.4. Sedimentation rates

The age-depth curves show upward-increasing sedimentation rates from Unit CSK3A to Unit CSK1A, with prominent inflections at the bases of Units CSK2 and CSK1B (Fig. 3). Taking real (variably compacted) thicknesses, 380 m of sediment have accumulated in the Anhydros Basin, and 480 m in the Anafi Basin, over the last 1.8 Ma. Separating the volcanic and non-volcanic inputs (neglecting any dispersed volcanic contribution in the background intervals), and decompacting the nonvolcanic sediment using shipboard bulk density data (Fig. 5e-f), the sedimentation rates for non-volcanic sediment are 9 – 14 cm kyr⁻¹ in Unit CSK3A and 12 – 18 cm kyr⁻¹ in Units CSK2 to CSK1A, reflecting the similar sedimentation histories of the two basins (Fig. 5c-d). These rates of background marine sedimentation resemble those measured in shallow gravity cores in the Aegean Sea surrounding, and east of, Santorini (averaging about 3 – 10 cm kyr⁻¹; Kutterolf et al., 2021). The time-averaged volcanic sedimentation rates in the two basins, essentially zero until 765 ka, are 25 - 40 cm kyr⁻¹ from 765 to 0 ka and 90 -140 cm kyr⁻¹ over the last 186 kyr (Fig. 5a-b).

5. Discussion

5.1. Eruption-fed megabeds in a volcanic rift system

While the rift basins contain numerous cm-thin tephra layers of probable fallout origin, several of the thickest volcanic layers (Figs. 2 e-f, S7) can be classified as volcaniclastic megabeds (Druitt et al., 2024b; Metcalfe et al., 2025). Based on chemical homogeneity, paucity of strong internal reflections, and lack of internal bioturbation, we interpret each megabed as having been emplaced rapidly by an eruption or shortly afterwards by remobilization of a primary deposit. This rapid deposition could have occurred by submarine gravity flows, fallout through the water column, and sinking of pumice rafts (Freundt et al., 2023). Megabeds thicker than a few meters are interpreted as the deposits from pyroclastic currents (from either subaerial or submarine vents) that entered the water column and, by entraining sea water, transformed into water-supported gravity flows (Clare et al., 2023; Cas et al., 2024). This interpretation is based on the fact that many of the Santorini eruptions that generated submarine megabeds in our cores are known from onland studies to have discharged voluminous pyroclastic currents into the sea (Druitt et al. 1999), as did the Kos Plateau Tuff eruption (Allen, 2001). The thickest megabeds are the Kos Plateau Tuff (210 m) and the Archaeos Tuff (~50 m) at Site U1592, and Lower Pumice 2 (38 m) at Site U1589 (Fig. 2 e-f). The Archaeos and Kos Plateau megabeds have been described in detail by Druitt et al. (2024a) and Metcalfe et al. (2025), respectively. Since the climactic phases of CFSEs typically last a few days or less, perhaps followed by several years to decades of remobilization, emplacement of each megabed was instantaneous on a geological timescale.

The prominence of megabeds in the SATZ basins is in marked contrast with sedimentation in most non-volcanic rifts. Although major re-sedimentation events due to flood input, slope instability or tsunami passage can produce megabeds, most sediment accumulation in non-volcanic rifts occurs incrementally (e.g., Gawthorpe et al., 2022). Many volcanic rifts are characterized by lava effusion and high supply rates of volcaniclastic material (Hutchison et al., 2016; Chen et al., 2022). The SATZ is an example of a rift system hosting CFSE volcanoes that generate huge, eruption-fed submarine deposits (Cas et al., 2024).

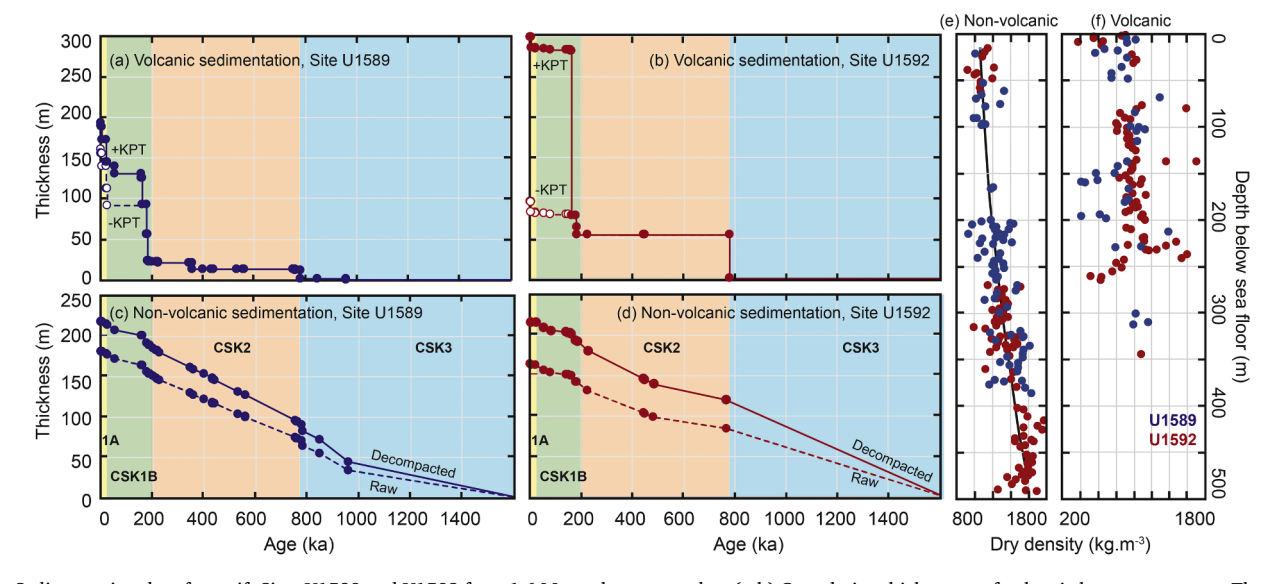


Fig. 5. Sedimentation data from rift Sites U1589 and U1592 from 1.6 Ma to the present day. (a-b) Cumulative thicknesses of volcanic layers versus age. The data are shown including and excluding the Kos Plateau Tuff (KPT), which does not derive from Santorini-Kolumbo. (c-d) Cumulative thicknesses of non-volcanic sediments versus age, both raw and decompacted. (e-f) Sediment dry density data from shipboard moisture and density measurement database (Druitt et al., 2024b). Non-volcanic sediments compact with burial, whereas volcanic products do not. The black line on (e) is a best fit polynomial to the non-volcanic sediment data (both sites combined) for dry bulk density (kg m $^{-3}$), $0.0015D^2 + 0.3965D + 1059.3$, where D is depth in meters, that was used to decompact the non-volcanic sediment thicknesses in (c-d).

Such gravity flows can travel over a hundred km from source and re-mould the seafloor landscape by erosion and by infilling of bathymetric troughs on an arc-wide scale, as shown by the Kos Plateau Tuff ash megabed in the Anafi Basin (Metcalfe et al., 2025).

5.2. Rift subsidence history

The new data allow us to revisit the published subsidence models for the Anhydros and Anafi basins based on seismic stratigraphy (Preine et al., 2022a). The sedimentation rates and stratigraphies of the two rift basins show that they have had similar histories of development since the onset of subsidence >2 Ma (Figs. 2 and 3). Using the thicknesses of sediment in each basin, the time-averaged subsidence rates since 1.8 Ma in the Anhydros and Anafi Basins have been 21 cm kyr⁻¹ and 27 cm kyr⁻¹, respectively (the higher rate of the Anafi Basin possibly being due to its greater thickness of volcanic megabeds (Fig. S9), lower elevation, and larger size; Nomikou et al., 2018). However, the subsidence may have been non-uniform, with a phase of accelerated rifting recorded by the seismic reflection onlap surface (Fig. 3a-b). Preine et al. (2022a) proposed that this onlap corresponds to a phase of rapid extension during which sedimentation failed to keep up with subsidence. The IODP data support this interpretation by showing that following the extension

event the rift basins were deep enough to accommodate a thick sequence of rapidly emplaced CFSE megabeds. This is particularly the case in the Anafi Basin where 235 m of ash was emplaced over 25 kyr (from 186 to 161 ka) and 210 m of ash from the Kos Plateau Tuff eruption was deposited in a single, geologically instantaneous event (Metcalfe et al., 2025). The Anafi basin must therefore have been >200 m deep, and the Anhydros Basin >100 m deep, to accommodate these megabeds. We therefore infer that during extension the basins became starved of sediment and subsequently acted as depocenters for eruption-fed gravity flows. These conclusions remain valid even when we take into account glacio-eustatic sea level changes, with minima of -80 to -120 m over the last 500 kyr (Grant et al., 2014).

We summarize the development of the Anhydros and Anafi Basins in three stages (Fig. 6): **Stage 1** (*Sedimentation* \approx *subsidence*): following the onset of rifting at >2 Ma, the sedimentation of Units CSK3 and CSK2 probably approximately kept up with subsidence, although transient fluctuations were likely. **Stage 2** (*Sedimentation* < *subsidence*): the rifting rate accelerated, and the basins deepened because sedimentation of Unit CSK2 could no longer keep up with subsidence. **Stage 3** (*Sedimentation* > *subsidence*): the deep basins formed during Stage 2 acted as depocenters into which pyroclastic currents of the Santorini TPF and Kos CFSEs poured, forming thick volcanic megabeds (Units CSK1B and

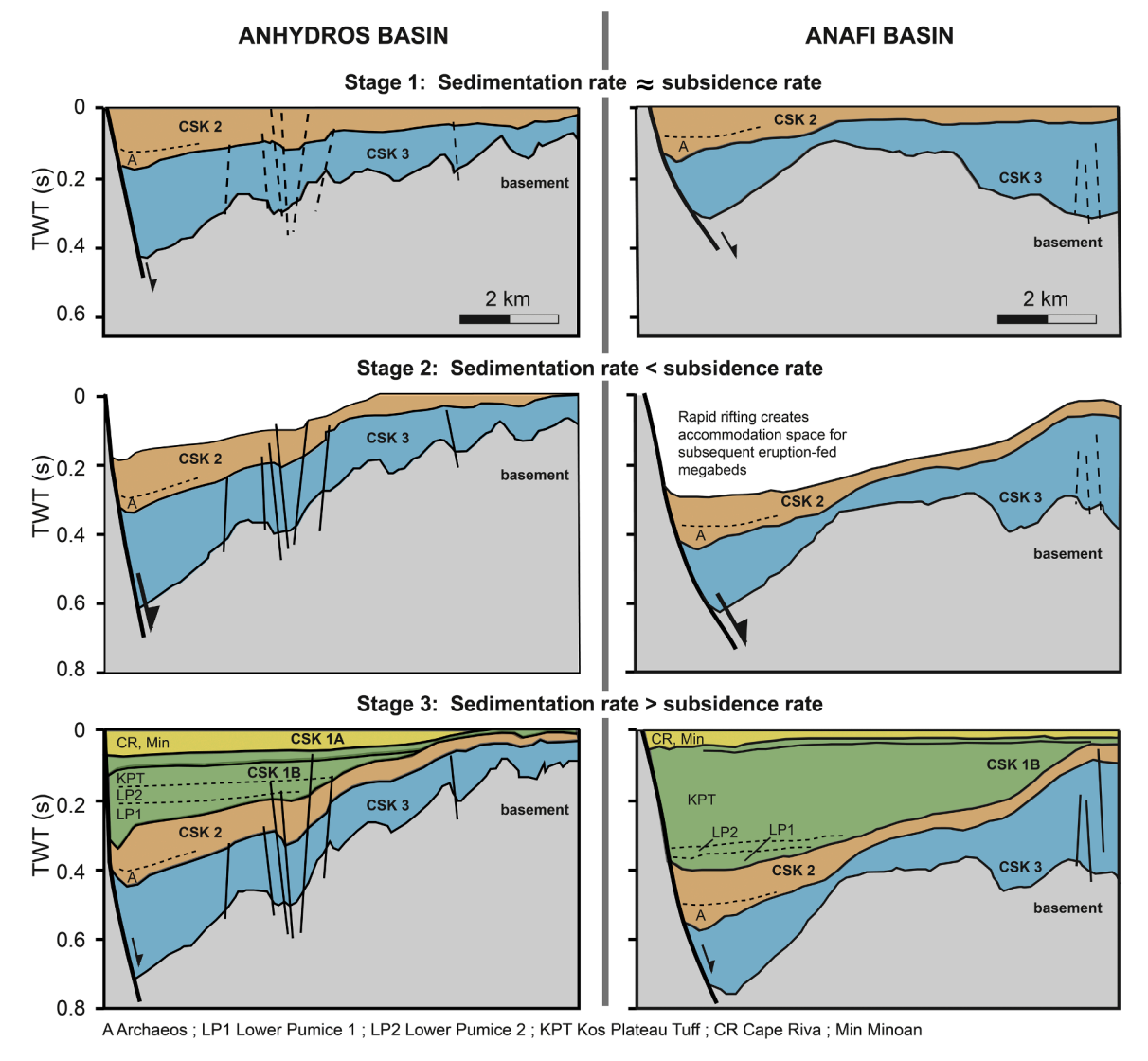


Fig. 6. Three stages in the development of the Anhydros and Anafi Basins described in the text, reconstructed from seismic sections and the drill core analysis. The reconstructions are based on successively flattening the top of each unit, as in Preine et al. (2022a). The colors of the chronostratigraphic units are the same as in Figs. 2c-d and 3a-c.

CSK1A). The seismic reflection onlap surface is interpreted as the combined product of (1) the existence of deep, rapidly subsiding basins, and (2) a change in sedimentation style from normal marine sediments (and thin tephra layers) to large, bathymetry-filling gravity flows. Subsidence rate during Stage 3 was insufficient to strongly tilt the CFSE megabeds of the Anhydros Basin, the top surfaces of which remain subhorizontal (Fig. 2). However, updrag of Unit CSK1B against the master fault of the Anafi half-graben (Fig. 2d) shows that significant subsidence continued in that basin during Stage 3 (Preine et al. 2022a).

Since sedimentation rate in the rifts increased with time during emplacement of Units CSK3A and CSK2 (Figs. 3 and 5), basin deepening during Stage 2 must have been due to increased subsidence rate, not decreased sedimentation rate. The duration of Stage 2 is not well constrained. Preine et al. (2022a) presented arguments based on the nature of internal seismic reflections that the transition from Stage 1 to Stage 2 was rapid, and that Stage 2 involved a well-defined, transient increase in extension rate or 'rift pulse' that possibly lasted several tens of thousands of years prior to the onset of caldera-forming eruptions of the TPF at ~250 ka. However, a more gradual acceleration of extension rate from Stage 1 to Stage 2 cannot be ruled out. In what follows we refer to Stage 2 as a phase of rapid rifting, 'rapid' meaning relative to local sedimentation rate and not neccessarily relative to rifts globally. Precise subsidence-time curves for the Anhydros and Anafi Basins await full structural re-evaluation of the rift basins in the light of IODP core-seismic integration.

5.3. Volcanic history of Santorini recorded by the rift successions

The results confirm the explosive volcanic record of Santorini known from onland studies and provide new insights.

First, the earliest tephra layer with Ancient Santorini chemistry at our rift sites is dated at 821 ka (Tephra K), older than the earliest volcanics dated onland (~650 ka; Druitt et al., 1999). This confirms published assertions that the onset of SATZ rifting (>2 Ma) preceded volcanism at Santorini and is consistent with the presence of an ancient 'proto-Anhydros' Basin buried beneath the volcano (Heath et al., 2019; Preine et al., 2022a). However, the presence of an even earlier tephra layer (Tephra L; 918 ka) with a high-K signature, as well as a 2.4-m-thick pumice layer ~1.6 Myr old recovered at IODP Expedition 398 Site U1600 (Fig. 1a; Druitt et al., 2024b), shows that one or more other volcanic centres already existed in the area before the eruption of Tephra K. It is also possible that Christiana Volcano, which was active until ~1.6 Ma (Preine et al., 2022a), partly predated opening of the SATZ.

Second, the earliest products of Modern Santorini (Tephra Series I) date from about 577 ka, broadly consistent with onland dating (530 ka; Druitt et al., 1999). A package of rhyolitic tephra layers with trace element signatures intermediate between those of Ancient and Modern Santorini (Tephra Series J) is dated 699 – 726 ka.

Third, the magma output rate and frequency of highly explosive eruptions during the TPF period exceeded those of the first $\sim\!300$ kyr years of Modern Santorini's history, as reflected in the great thickness of basin-hosted megabeds from the TPF eruptions (Fig. 5a-b). Between 30 and 50 % of the basin fills accumulated in just one tenth of the lifetimes of the rifts.

5.4. Rift modulation of caldera volcanism?

We now focus on the possible relationships of lithospheric rifting to the transition to caldera-forming silicic eruption (CFSE) activity at Modern Santorini ~250 kyr ago. By ground-truthing the seismic stratigraphy of Preine et al. (2022a), and integrating volcanic, sedimentary and tectonic histories (Fig. 7), we have shown the existence of a single major seismic reflection onlap surface and have confirmed that the majority of the TPF eruptions (and the Kos Plateau Tuff) lie directly above that onlap. We have also shown that these deposits (Units CSK1A

and CSK1B) consist largely of stacked gravity-flow-emplaced megabeds, representing a marked change in sedimentation mechanism from the nonvolcanic sediments and lesser tephra layers (Unit CSK2) beneath the onlap surface. This opens up two possible interpretations of the relationship between rifting and CSFE volcanism.

Model 1. In this interpretation the transition of Modern Santorini to CFSE activity was driven purely by internal magmatic processes and was unrelated to tectonics. Subsidence of Stage 2 progressively deepened the rift basins until they formed bathymetric troughs. Then, when Santorini became highly explosive, the basins simply acted as passive receptacles for the pyroclastic gravity flows, whose thick deposits onlapped the basin margins in a manner analogous to a terrestrial pyroclastic flow filling a valley (e.g., Cas et al. 2024).

Model 2. In this interpretation the transition to CFSE activity was the result of prolonged extension and a phase of rapid subsidence and basin deepening (Stage 2; Preine et al. 2022a), with a direct relationship between rifting and explosive volcanism. The question arises in Model 2 as to whether rifting caused the CFSE volcanism or whether an increased crustal magmatic activity prior to the onset of the TPF triggered the phase of rapid rifting by thermally weakening the lithosphere, lubricating faults, and accommodating strain (Brune et al., 2023). Since Plio-Quaternary rifting in the central and southeastern Aegean is regionally driven (Jolivet et al., 2013; Sternai et al., 2014), we favour that in Model 2 the elevated levels of crustal magmatism that drove the TPF were the result of rifting, not vice versa.

While we cannot definitively exclude Model 1, the location of Santorini in the western Anhydros Basin, the evidence for rapid rift extension, and the well documented influence of tectonics on volcanism in the area (Kokkalas and Aydin, 2012; Hooft et al., 2017; Heath et al., 2019, 2021; Preine et al. 2022a; Drymoni et al., 2022) lend support to Model 2. We therefore explore three mechanisms by which rifting may have modulated the transition of Modern Santorini to CSFE activity (Fig. 8).

Change in mantle melt extraction. Rapid rifting prior to ~250 ka may have increased the flux of mantle-derived melts, fluids and heat to the transcrustal magmatic system. Two observations support a change in mantle supply to Modern Santorini at this time. First, the increased eruption rate of the TPF compared to the preceding period (Fig. 1b) implies an increased flux of basalt into the crust. Increased mantle flux was necessary to provide the extra mass and heat to the transcrustal magmatic system to generate the >120 km³ of chemically evolved melts erupted as the TPF, an output possibly several times higher than that during the preceding Peristeria period (Figs. 1b and 5 a-b). Second, magmas of the TPF are poorer in incompatible elements such as K, Rb, Th and Zr than those of the preceding Peristeria Volcano, suggesting a change in the nature of the incoming parental melts (Fig. S10; Huijsmans et al., 1988; Druitt et al., 1999). One explanation for increased mantle supply might have been an increase in the degree of mantle melting due to lithospheric thinning. However, slowly extending rifts like the SATZ (<few mm yr⁻¹; Feuillet, 2013) do not generate large amounts of decompression melting in thermomechanical models at the mantle potential temperatures beneath Santorini (1350 – 1440°C; Flaherty et al., 2022) (see figure 9 in Fioraso et al., 2024). Several kilometers of localized, extension-driven mantle upwelling beneath the volcano would therefore have been necessary to generate even a few % of additional melting (Sternai, 2020). More likely, transient changes in asthenospheric flow rates and patterns accompanying rifting increased the rate of melt extraction from more refractory, higher-temperature regions of the mantle wedge (e.g., Leeman 2020), supplementing the input from more enriched, fluid-fluxed regions and raising the total supply of basalt (e.g., Hutchison et al., 2016).

Increased melt percolation through the transcrustal magmatic system. Rapid rifting may also have caused an increase in crustal shearing, rock permeability, shear-induced melt segregation, and gravitational instabilities in magmatic mushes of the transcrustal magmatic system (Kohlstedt and Holtzman, 2009; Sparks et al., 2019; Weinberg et al., 2021). Given favorable stress conditions, these effects may have

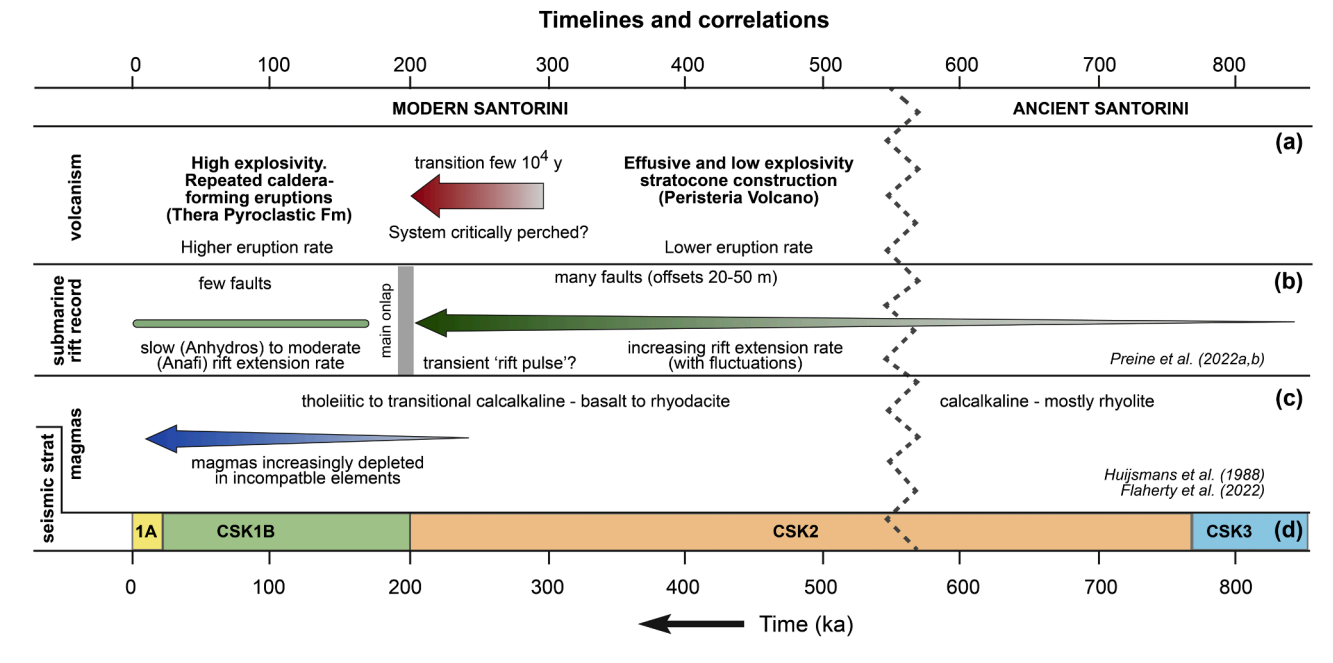


Fig. 7. Schematic summary of major volcanic and tectonic events. (a) Volcanic activity. (b) Rifting record from core-seismic integration. (c) Geochemical features of Santorini magmas from previous studies. (d) Chronostratigraphic stratigraphy in the submarine cores. Source references are given on the figure.

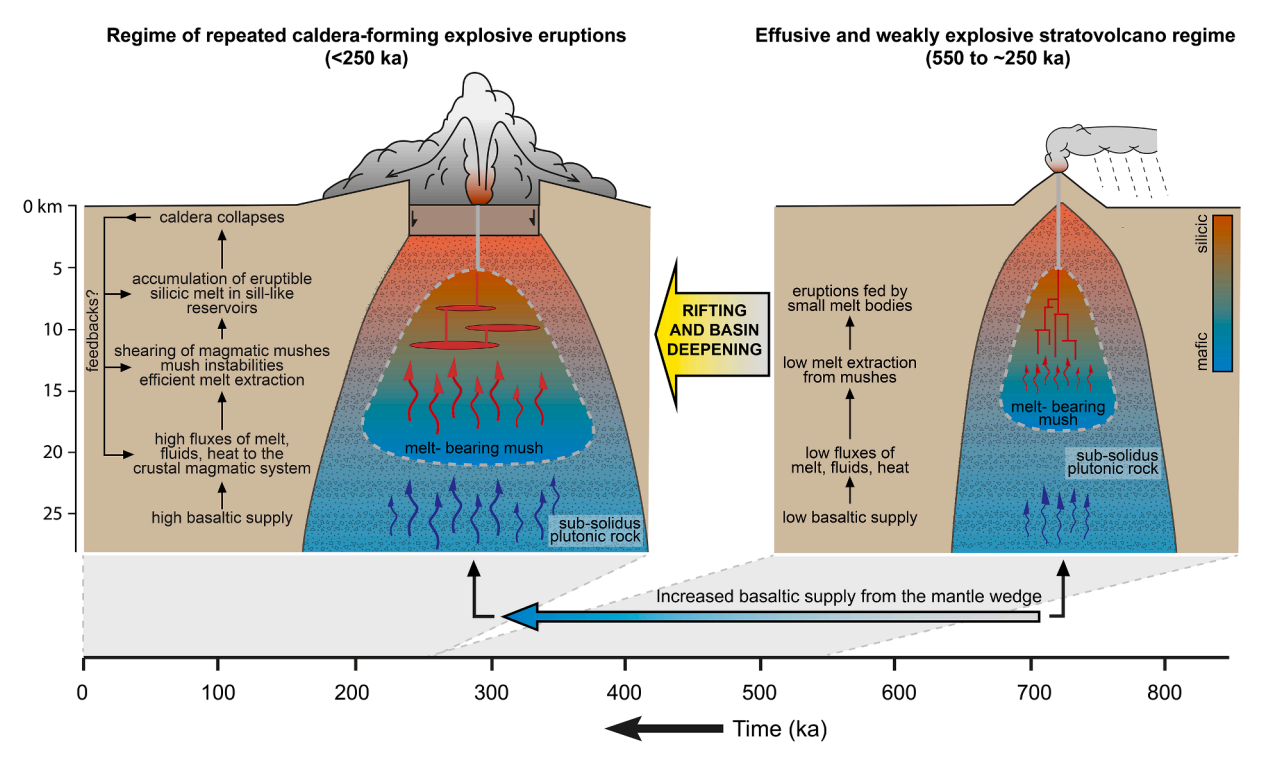


Fig. 8. Schematic (Model 2) for the modulation of volcanic activity at Modern Santorini by the phase of accelerated rifting that took place between about 300 and 250 ka. Subsolidus plutonic rock of the transcrustal magmatic system is shown patterned in pale colours and melt storage regions are shown in stronger colours, with blue for mafic compositions and red for silicic compositions. The rifting is interpreted as having increased the fluxes of melts, fluids and heat from the mantle and through the transcrustal magmatic system, driving a transition from predominantly effusive and weakly explosive andesitic behavior to strongly explosive activity with repeated caldera-forming silicic eruptions. The blue arrows depict ascent of parental basalt, and the red arrows depict movement of silicic melts through the transcrustal crystal mushes.

increased the upward flow of silicic/intermediate melts and fluids through the transcrustal magma reservoir of Santorini, promoting formation of the large upper crustal lenses of gas-charged eruptible melt necessary to feed CFSEs (Flaherty et al., 2018).

Changes in magma storage architecture. A third possibility is that

prolonged rifting and basin deepening caused a change in the magma reservoir architecture of the transcrustal magmatic system. Stresses induced by deepening volcanic rifts influence magma storage architecture by changing the balance between regional and unloading stress components (Ferrante et al., 2024). As a rift deepens, the minimum

principal stress can rotate towards the vertical, promoting development of complexes of stacked sills in the middle to lower crust. Top-down crustal stress changes due to progressive deepening of the western Anhydros Basin may therefore have favored a transition at Santorini from dyke-dominated magma ascent to the development of stacked sills that could then have trapped the incoming basalt and led to thermal runaway. Repeated transient unloading due to caldera collapses could then have maintained a sill-dominated architecture through feedback effects, while also maintaining high melt fluxes through the magmatic system, possibly explaining the continuation of CFSE-dominated activity into the Holocene (Corbi et al. 2015).

In summary, Model 2 envisages that a rifting-induced increase in flow of melts, fluids and heat into, and through, the transcrustal magmatic system, coupled with changes in magma reservoir architecture, may have amplified the internal magmatic processes at Santorini and driven it $\sim\!250\,\rm kyr$ ago from an andesitic stratovolcano into a regime of repeated CFSE activity (Fig. 8). The effects of tectonic forcing would have been facilitated if, following over 300 kyr of activity of Modern Santorini from 550 to 250 ka (plus the additional $\sim\!300\,\rm kyr$ of Ancient Santorini), the transcrustal magmatic system was already hot and primed for thermomechanical runaway. If the phase of rapid rifting (Stage 2 of Fig. 6) lasted at least several tens of thousands of years, then this time was available for the transcrustal magmatic system to react to it before the first CFSE of Modern Santorini at 186 ka (Figs. 1b and 7).

Distinguishing definitively between Models 1 and 2 will require detailed re-evaluation of the basin evolution in the light of the new coreseismic integration. However, a correlation of eruptive events across the South Aegean Volcanic Arc provides additional weight in favour of Model 2, as now described.

5.5. A flare-up of caldera-forming activity on the South Aegean Volcanic Arc

The western sector of the volcanic arc is characterized by small, commonly monogenetic centers, whereas the central (Christiana–Santorini–Kolumbo) and eastern (Kos–Nisyros–Yali) sectors are both characterized by composite volcanoes with calderas (Vougioukalakis et al., 2019). This suggests that higher mantle supply rates, and/or crustal stress conditions, are more favourable to the formation of calderas in the central and eastern sectors than further west. Interestingly, the two caldera systems – Santorini and Kos – lie in mature rift systems, reinforcing the relationship between rifting and explosive activity. The rift system hosting the Kos caldera is oriented WSW-ENE and, like the SATZ, is of late Pliocene to Pleistocene age (Papanikolaou et al., 2018).

It is notable that the Kos Plateau Tuff eruption, the largest eruption of the Kos volcanic centre since the $\sim\!500$ ka Kefalos eruptions (Bachmann et al., 2019), occurred at 161 ka just after the Lower Pumice pair of CFSEs (186 and 177 ka) at Santorini. Moreover, the Kos caldera has remained in an explosive state to the present day, with at least two >10 km³ explosive eruptions from Nisyros and Yali Volcanoes on the rim of the Kos caldera (Kutterolf et al., 2021). This raises the possibility of broad synchronizations between the rift-hosted Santorini and Kos magmatic systems, and a 0.2 Ma flare-up of caldera-forming volcanism in the central and eastern sectors of the volcanic arc. The connection is likely to have arisen from the same plate-wide stresses driving rifting at both systems (Jolivet et al., 2013), and from the Kos-Nisyros-Yali magmatic system having interacted with its rift environment in a similar manner to Modern Santorini, as inherent in Model 2 above.

An ignimbrite flare-up is a period of abnormally high explosive activity along a segment of volcanic arc or continental rift, such as the Central Volcanic Zone of the Andes (de Silva et al., 2015), the Taupō Volcanic Zone of New Zealand (Gravely et al., 2016), or the East African Rift (Hutchison et al., 2016). Flare-ups occur on a range of timescales, from 10^4 to $\geq 10^7$ yrs, and can explosively discharge up to 10^3 - 10^4 km³ of silicic magma (Gravely et al., 2016). The CFSE flare-up at Santorini and Kos-Nisyros-Yali volcanic fields is small relative to other examples

on a global scale in terms of timescales (a few $10^4\,\mathrm{yr}$) and total (Santorini TPF plus Kos) volumes of erupted magma (\sim 200 km³). However, it is similar in spatial, temporal and volume scales to that which took place in the rift valley of Ethiopia in the Middle Pleistocene (Hutchison et al., 2016). Our integrated core-seismic dataset suggests that the flare-up at Santorini and Kos may have been triggered by a phase of accelerated, regional rifting, and that the magmatic systems took at least several tens of thousands of years to react to the changes in lithospheric stresses and mantle supply. These findings show that the well-known multiscale nature of volcanic arc tempos (de Silva et al., 2015), and the effects of tectonic forcing, may extend down to the small temporal (10^4 - $10^5\,\mathrm{yr}$) and volume ($10^2\,\mathrm{km}^3$) scales typical of individual caldera cycles at arc volcanoes (Bouvet de Maisonneuve et al., 2021).

6. Conclusions

- The close association of caldera volcanism with lithospheric rifting in the central and eastern sectors of the South Aegean Volcanic Arc makes the region a natural laboratory for investigating volcanotectonic couplings at calderas.
- 2. IODP Expedition 398 deep-drilled the volcano-sedimentary fills of the rift basins that lie northeast of, and underneath, Santorini (Santorini-Amorgos Tectonic Zone), ground-truthing existing seismic stratigraphy and generating a unique, high-resolution, core-seismic integration record of volcanic activity and lithospheric extension on a volcanic arc. The results reveal a possible example of rift modulation of an arc magmatic system on the 10⁴ 10⁵ yr timescales typical of caldera cycles.
- 3. Regionally-driven rift extension began >2 Ma, then accelerated into a rapid phase during which the marine basins deepened because subsidence outpaced sedimentation. These bathymetric troughs then subsequently acted as depocenters for thick sequences of lapilli-ash megabeds fed by caldera-forming eruptions of Santorini (Thera Pyroclastic Formation) and the Kos Plateau Tuff eruption of Kos Volcano.
- 4. The phase of accelerated rifting may have pushed Modern Santorini ~250 ka from a regime of effusive and weakly explosive behavior typical of andesitic stratovolcanoes into its present-day highly explosive, caldera-forming state. The rifting may have amplified the normal internal processes and feedbacks of magma ascent, storage and eruption by (i) increasing the flow of magmatic melts, fluids and heat through the transcrustal magmatic system, (ii) modifying the architecture of magma storage, and (iii) driving the system into thermomechanical runaway. Repeated transient unloading of the volcanic plumbing system by caldera collapses may have helped sustain the highly explosive activity into the Holocene.
- 5. Broadly simultaneous transitions of the rift-hosted Santorini and Kos volcanic fields into caldera-forming activity about 0.2 million years ago suggest that the eruptive states of the two magmatic systems are linked by plate-scale lithospheric stresses.

Funding

This research was supported by IODP (participation of shipboard scientists on IODP Expedition 398), IODP France (A.Me and T.D), GEOWARN project contract no: IST-1999- 12310 (P.N.), Seafloor mapping of the Santorini-Amorgos region OCE-1548026 (P.N.), German Research Foundation (DFG) IODP priority programme KU2685/17-1, project number: 527924707 (S.K. and K.P.) and German Science Foundation grant numbers 434763330 and 506199584 (C.H. and J.P.).

CRediT authorship contribution statement

Abigail Metcalfe: Writing – original draft, Writing – review & editing, Data curation. **Tim Druitt:** Writing – original draft, Writing – review & editing, Data curation, Conceptualization. **Katharina Pank:**

Writing – review & editing, Data curation. Steffen Kutterolf: Writing – review & editing, Data curation, Conceptualization. Jonas Preine: Writing - review & editing, Data curation, Conceptualization. Sarah Beethe: Writing - review & editing, Data curation. Axel Schmitt: Writing - review & editing, Data curation. Christian Hübscher: Writing - review & editing, Data curation, Conceptualization. Paraskevi Nomikou: Writing - review & editing, Data curation, Conceptualization. Thomas A. Ronge: Writing - review & editing, Project administration. Carole Berthod: Data curation. Hehe Chen: Data curation. Shun Chiyonobu: Data curation. Acacia Clark: Data curation. Susan DeBari: Data curation. Ralf Gertisser: Writing - review & editing, Data curation. Raymond Johnston: Data curation. Olga Koukousioura: Data curation. Michael Manga: Writing - review & editing, Data curation. Molly McCanta: Data curation. Iona McIntosh: Data curation. Ally Peccia: Data curation. Masako Tominaga: Data curation. Yuzuru Yamamoto: Data curation. Adam Woodhouse: Data curation. Alexis Bernard: Data curation. Tatiana Fernandez Perez: Data curation. Christopher K. Jones: Data curation. Kumar Batuk Joshi: Data curation. Günther Kletetschka: Writing - review & editing, Data curation. Antony Morris: Data curation. Paraskevi Polymenakou: Data curation. Xiaohui Li: Data curation. Dimitrios Papanikolaou: Funding acquisition. David Pyle: Writing - review & editing. Pietro Sternai: Writing - review & editing.

Declaration of competing interest

The authors declare that they have no known competing financial interests or personal relationships that could have appeared to influence the work reported in this paper.

Acknowledgements

This research used samples and data provided by the International Ocean Discovery Program (IODP). We thank the technical staff of the *JOIDES Resolution* for their efforts in attaining the scientific goals of Expedition 398. Special gratitude goes to Bill Rheinehart, Chieh Peng and colleagues in helping us overcome many obstacles and to Katerina Petronotis and the leadership of IODP for their support. We thank the member organizations of IODP for financial aid, and the Municipality of Thera for help in preparing for the expedition. Jean-Luc Devidal provided greatly appreciated technical support in microbeam analysis. Derek Keir and an anonymous reviewer provided helpful suggestions for improving the manuscript. This is contribution number 716 of the ClerVolc program of Clermont-Auvergne University.

Supplementary materials

Supplementary material associated with this article can be found, in the online version, at doi:10.1016/j.epsl.2025.119633.

Data availability

High-resolution seismic profiles from cruise POS538 can be accessed from Pangea at https://doi.org/10.1594/PANGAEA.956579. A selection of vintage seismic profiles can be found in the marine geoscience data system (MGDS) at https://doi.org/10.26022/IEDA/327525 and https://doi.org/10.26022/IEDA/331028.

References

- Allen, S.R., 2001. Reconstruction of a major caldera-forming eruption from pyroclastic deposit characteristics: Kos Plateau Tuff, eastern Aegean Sea. J. Volcanol. Geotherm. Res. 105, 141–162.
- Autumn, K.R., Hooft, E.E.E., Toomey, D.R., 2025. Exploring mid-to-lower crustal magma plumbing of Santorini and Kolumbo Volcanoes using PmP tomography. Geochem. Geophys. Geosys 26, e2025GC012170. https://doi.org/10.1029/2025GC012170.

- Bachmann, O., Huber, C., 2016. Silicic magma reservoirs in the Earth's crust. Am. Miner. 101, 2377–2404. https://doi.org/10.2138/am-2016-5675.
- Bachmann, O., Allen, S.R., Bouvet de Maisonneuve, C., 2019. The Kos–Nisyros–Yali Volcanic field. Elements 15, 191–196. https://doi.org/10.2138/
- Berryman, K., Villamor, P., Nairn, I., Begg, J., Alloway, B.V., Rowland, J., Lee, J., Capote, R., 2022. Volcano-tectonic interactions at the southern margin of the Okataina Volcanic Centre, Taupo Volcanic Zone, New Zealand. J. Volcanol. Geotherm. Res. 427, 107552. https://doi.org/10.1016/j.jvolgeores.2022.10755
- Bouvet de Maisonneuve, C., Forni, F., Bachmann, O., 2021. Magma reservoir evolution during the build up to and recovery from caldera-forming eruptions – a generalizable model? Earth Sci. Rev. 218, 103684. https://doi.org/10.1016/j. earsgirev.2021.103684
- Brune, S., Kolawole, F., Olive, J.-A., Stamps, D.S., Buck, W.R., Buiter, S.J.H., Furman, T., Shillington, D.J., 2023. Geodynamics of continental rift initiation and evolution. Nat. Rev. Earth Env. 4, 235–253. https://doi.org/10.1038/s43017-023-00391-3.
- Burns, D.H., de Silva, S.L., Tepley, F., Schmitt, A.K., Loewen, M.W., 2015. Recording the transition from flare-up to steady-state arc magmatism at the Purico-Chascon volcanic complex, northern Chile. Earth Planet. Sci. Lett. 422, 75–86. https://doi. org/10.1016/j.epsl.2015.04.002.
- Cas, R., Giordano, G., Wright, J.V., 2024. Volcanology. Processes, deposits, geology and resources. Springer, p. 1833.
- Cashman, K.V., Sparks, R.S.J., Blundy, J.D., 2017. Vertically extensive and unstable magmatic systems: a unified view of igneous processes. Science 355, eaag3055. https://doi.org/10.1126/science.aag3055.
- Cassidy, M., Mani, L., 2022. Huge volcanic eruptions: time to prepare. Nature 608, 469–471. https://doi.org/10.1038/d41586-022-02177-x.
- Chen, H., Zhu, X., Gawthorpe, R.L., Wood, L.J., Liu, Q., Li, S., Shi, R., Li, H., 2022. The interactions of volcanism and clastic sedimentation in rift basins: insights from the palaeogene-neogene shaleitian uplift and surrounding sub-basins, Bohai Bay Basin. China. Basin Res. 34, 1084–1112.
- Clare, M.A., Yeo, I.A., Watson, S., Wysoczanski, R., Seabrook, S., Mackay, K., Hunt, J.E., Lane, E., Talling, P.J., Pope, E., Cronin, S., Ribó, M., Kula, T., Tappin, D., Henrys, S., de Ronde, C., Urlaub, M., Kutterolf, S., Fonua, S., Panuve, S., Veverka, D., Rapp, R., Kamalov, V., Williams, M., 2023. Fast and destructive density currents created by ocean-entering volcanic eruptions. Science 381, 1085–1092. https://doi.org/10.1126/science.adi3038.
- Corbi, F., Rivalta, E., Pinel, V., Maccaferri, F., Bagnardi, M., Acocella, V., 2015. How caldera collapse shapes the shallow emplacement and transfer of magma in active volcanoes. Earth Planet. Sci. Lett. 431, 287–293. https://doi.org/10.1016/j. epsl.2015.09.028.
- Crutchley, G.J., Karstens, J., Preine, J., Hübscher, C., Fossen, H., Kühn, M., 2023. Extensional faulting around Kolumbo Volcano, Aegean Sea—Relationships between local stress fields, fault relay ramps, and volcanism. Tectonics 42, e2023TC007951. https://doi.org/10.1029/2023TC007951.
- Degruyter, W., Huber, C., Bachmann, O., Cooper, K.M., Kent, A.J.R., 2016. Magma reservoir response to transient recharge events: the case of Santorini volcano (Greece). Geology 44, 23–26. https://doi.org/10.1130/G37333.1.
- De Silva, S.L., Riggs, N.R., Barth, A.P., 2015. Quickening the pulse: fractal tempos in continental arc magmatism. Elements 11, 113–118. https://doi.org/10.2113/gselements.11.2.113.
- Druitt, T.H., Edwards, L., Mellors, R.M., Pyle, D.M., Sparks, R.S.J., Lanphere, M., Davies, M., Barreirio, B., 1999. Santorini volcano. Geol. Soc. Mem. 19.
- Druitt, T., Kutterolf, S., Ronge, T.A., Hübscher, C., Nomikou, P., Preine, J., Gertisser, R., Karstens, J., Keller, J., Koukousioura, O., Manga, M., Metcalfe, A., McCanta, M., McIntosh, I., Pank, K., Woodhouse, A., Beethe, S., Berthod, C., Chiyonobu, S., Chen, H., Clark, A., DeBari, S., Johnston, R., Peccia, A., Yamamoto, Y., Bernard, A., Perez, T.F., Jones, C., Joshi, K.B., Kletetschka, G., Li, X., Morris, A., Polymenakou, P., Tominaga, M., Papanikolaou, D., Wang, K.-L., Lee, H.-Y., 2024a. Giant offshore pumice deposit records a shallow submarine explosive eruption of ancestral Santorini. Comm. Earth Env. 5, 24. https://doi.org/10.1038/s43247-023-01171-z.
- Druitt, T.H., Kutterolf, S., Ronge, T.A., 2024b. Hellenic Arc Volcanic Field. In: Proceedings of the International Ocean Discovery Program Expedition Reports, p. 398. https://doi.org/10.14379/iodp.proc.398.2024.
- Drymoni, K., Browning, J., Gudmundsson, A., 2022. Spatial and temporal volcanotectonic evolution of Santorini volcano. Greece. Bull. Volcanol. 84, 60. https://doi.org/10.1007/s00445-022-01566-4.
- Ferrante, G., Rivalta, E., Maccaferri, F., 2024. Spatio-temporal evolution of rift volcanism controlled top-down by a deepening graben. Earth Planet. Sci. Lett. 629, 118593. https://doi.org/10.1016/j.epsl.2024.118593.
- Feuillet, N., 2013. The 2011–2012 unrest at Santorini rift: stress interaction between active faulting and volcanism. Geophys. Res. Lett. 40, 3532–3537. https://doi.org/ 10.1002/grl.50516.
- Fioraso, M., Sternai, P., Olivetti, V., Balestrieri, M.L., Zattin, M., Cornamusini, G., 2024. Miocene climate cooling and aridification of Antarctica may have enhanced synextensional magmatism in the western Ross Sea. Glob. Planet. Change 240, 104538. https://doi.org/10.1016/j.gloplacha.2024.104538.
- Flaherty, T., Druitt, T.H., Tuffen, H., Higgins, M.D., Costa, F., Cadoux, A., 2018. Multiple timescale constraints for high-flux magma chamber assembly prior to the late Bronze Age eruption of Santorini (Greece). Contrib. Miner. Pet. 173, 75. https://doi.org/ 10.1007/s00410-018-1490-1.
- Flaherty, T., Druitt, T.H., Francalanci, L., Schiano, P., Sigmarsson, O., 2022. Temporal variations in the diversity of primitive melts supplied to the Santorini silicic magmatic system and links to lithospheric stresses. Contrib. Miner. Pet. 177, 79. https://doi.org/10.1007/s00410-022-01941-6.

- Freundt, A., Schindlbeck-Belo, J.C., Kutterolf, S., Hopkins, J.L., 2023. Tephra layers in the marine environment: a review of properties and emplacement processes. Geol. Soc. L. Spec. Publ. 520, 595–637. https://doi.org/10.1144/SP520-2021-50.
- Gawthorpe, R.L., Fabregas, N., Pechlivanidou, S., Ford, M., Collier, R.E.L., Carter, G.D., McNeill, L.C., Shillington, D.J., 2022. Late quaternary mud-dominated, basin-floor sedimentation of the Gulf of Corinth, Greece: implications for deep-water depositional processes and controls on syn-rift sedimentation. Basin Res. 34, 1567–1600.
- Grant, K.M., Rohling, E.J., Ramsey, C.B., Cheng, H., Edwards, R.L., Florindo, F., Heslop, D., Marra, F., Roberts, A.P., Tamisiea, M.E., Williams, F., 2014. Sea-level variability over five glacial cycles. Nat. Comm. 5, 5076.
- Gravley, D.M., Deering, C.D., Leonard, G.S., Rowland, J.V., 2016. Ignimbrite flare-ups and their drivers: a New Zealand perspective. Earth Sci. Rev. 162, 65–82. https:// doi.org/10.1016/j.earscirev.2016.09.007.
- Heath, B.A., Hooft, E.E.E., Toomey, D.R., Papazachos, C.B., Nomikou, P., Paulatto, M., Morgan, J.V., Warner, M.R., 2019. Tectonism and its relation to magmatism around Santorini Volcano from upper crustal P wave velocity. J. Geophys. Res. Solid Earth 124, 10610–10629. https://doi.org/10.1029/2019JB017699.
- Heath, B.A., Hooft, E.E.E., Toomey, D.R., Paulatto, M., Papazachos, C.B., Nomikou, P., Morgan, J.V., 2021. Relationship between active faulting/fracturing and magmatism around Santorini: seismic anisotropy from an active source tomography experiment. J. Geophys Res.: Solid Earth 126, e2021JB021898.
- Hooft, E.E.E., Nomikou, P., Toomey, D.R., Lampridou, D., Getz, C., Christopoulou, M.-E., O'Hara, D., Arnoux, G.M., Bodmer, M., Gray, M., Heath, B.A., VanderBeek, B.P., 2017. Backarc tectonism, volcanism, and mass wasting shape seafloor morphology in the Santorini-Christiana-Amorgos region of the Hellenic Volcanic Arc. Tectonophys 712–713, 396–414. https://doi.org/10.1016/j.tecto.2017.06.005.
- Hübscher, C., Ruhnau, M., Nomikou, P., 2015. Volcano-tectonic evolution of the polygenetic Kolumbo submarine volcano/Santorini (Aegean Sea). J. Volcanol. Geotherm. Res. 291, 101–111. https://doi.org/10.1016/j.jvolgeores.2014.12.020.
- Hufstetler, R.S., Hooft, E.E., Toomey, D.R., VanderBeek, B.P., Papazachos, C.B., Chatzis, N., 2025. Seismic structure of the mid to upper crust at the Santorini-Kolumbo Magma System from joint earthquake and active source vp-vs tomography. Geochem. Geophys. Geosys 26, e2024GC012022.
- Hughes, G.R., Mahood, G.A., 2008. Tectonic controls on the nature of large silicic calderas in volcanic arcs. Geology 36, 627. https://doi.org/10.1130/G24796A.1.
- Huijsmans, J.P., Barton, M., Salters, V.J., 1988. Geochemistry and evolution of the calcalkaline volcanic complex of Santorini, Aegean Sea, Greece. J. Volcanol.Geotherm. Res. 34, 283–306.
- Hutchison, W., Fusillo, R., Pyle, D.M., Mather, T.A., Blundy, J.D., Biggs, J., Yirgu, G., Cohen, B.E., Brooker, R.A., Barfod, D.N., Calvert, A.T., 2016. A pulse of midpleistocene rift volcanism in Ethiopia at the dawn of modern humans. Nat. Comm. 7, 13192. https://doi.org/10.1038/ncomms13192.
- Jellinek, A.M., DePaolo, D.J., 2003. A model for the origin of large silicic magma chambers: precursors of caldera-forming eruptions. Bull. Volcanol. 65, 363–381. https://doi.org/10.1007/s00445-003-0277-y.
- Jolivet, L., Faccenna, C., Huet, B., Labrousse, L., Le Pourhiet, L., Lacombe, O., Lecomte, E., Burov, E., Denèle, Y., Brun, J.-P., Philippon, M., Paul, A., Salaün, G., Karabulut, H., Piromallo, C., Monié, P., Gueydan, F., Okay, A.I., Oberhänsli, R., Pourteau, A., Augier, R., Gadenne, L., Driussi, O., 2013. Aegean tectonics: strain localisation, slab tearing and trench retreat. Tectonophys 597–598, 1–33. https:// doi.org/10.1016/j.tecto.2012.06.011.
- Jutzeler, M., Clark, A.S., Manga, M., McIntosh, I., Druitt, T., Kutterolf, S., Ronge, T.A., 2025. Data report: coring disturbances in advanced piston cores from IODP expedition 398, Hellenic Arc Volcanic Field. In: Proceedings of the International Ocean Discovery Program, p. 398. https://doi.org/10.14379/iodp.proc.398.203.2025
- Karakas, O., Dufek, J., 2015. Melt evolution and residence in extending crust: thermal modeling of the crust and crustal magmas. Earth Planet. Sci. Lett. 425, 131–144. https://doi.org/10.1016/j.epsl.2015.06.001.
- Kohlstedt, D.L., Holtzman, B.K., 2009. Shearing melt out of the Earth: an experimentalist's perspective on the influence of deformation on melt extraction. Annu. Rev. Earth Planet Sci. 37, 561–593. https://doi.org/10.1146/annurev. earth.031208.100104.
- Kokkalas, S., Aydin, A., 2012. Is there a link between faulting and magmatism in the south-central Aegean Sea? Geol. Mag. 150, 193–224. https://doi.org/10.1017/ S0016756812000453.
- Kutterolf, S., Freundt, A., Druitt, T.H., McPhie, J., Nomikou, P., Pank, K., Schindlbeck-Belo, J.C., Hansteen, T.H., Allen, S.R., 2021. The medial offshore record of explosive volcanism along the central to eastern Aegean Volcanic Arc: 2. Tephra ages and volumes, eruption magnitudes and marine sedimentation rate variations. Geochem. Geophys. Geosys 22 e2021GC010011.
- Leeman, W.P., 2020. Old/new subduction zone paradigms as seen from the Cascades. Front. Earth Sci. 8, 535879. https://doi.org/10.3389/feart.2020.535879.
- McVey, B.G., Hooft, E.E.E., Heath, B.A., Toomey, D.R., Paulatto, M., Morgan, J.V., Nomikou, P., Papazachos, C.B., 2019. Magma accumulation beneath Santorini volcano, Greece, from P-wave tomography. Geology 48, 231–235. https://doi.org/ 10.1130/G47127.1.

- Metcalfe, A., 2025. Submarine ash megabed fed by far-traveled, shoreline-crossing pyroclastic currents from a large explosive volcanic eruption. Sci. Adv. 11, eads9642.
- Muirhead, J.D., Illsley-Kemp, F., Barker, S.J., Villamor, P., Wilson, C.J.N., Otway, P., Mestel, E.R.H., Leonard, G.S., Ellis, S., Savage, M.K., Bannister, S., Rowland, J.V., Townsend, D., Hamling, I.J., Hreinsdóttir, S., Smith, B., McGregor, R., Snowden, M., Shalla, Y., 2022. Stretching, shaking, inflating: volcanic-tectonic interactions at a rifting Silicic Caldera. Front. Earth Sci. 10, 835841. https://doi.org/10.3389/feart.2022.835841.
- Newhall, C., Self, S., Robock, A., 2018. Anticipating future Volcanic Explosivity Index (VEI) 7 eruptions and their chilling impacts. Geosphere 14, 572–603. https://doi. org/10.1130/GES01513.1.
- Nomikou, P., Hübscher, C., Ruhnau, M., Bejelou, K., 2016. Tectono-stratigraphic evolution through successive extensional events of the Anydros Basin, hosting Kolumbo volcanic field at the Aegean Sea. Greece. Tectonophys 671, 202–217. https://doi.org/10.1016/j.tecto.2016.01.021.
- Nomikou, P., Hübscher, C., Papanikolaou, D., Farangitakis, G.P., Ruhnau, M., Lampridou, D., 2018. Expanding extension, subsidence and lateral segmentation within the Santorini - Amorgos basins during quaternary: implications for the 1956 Amorgos events, central - south Aegean Sea. Greece. Tectonophys 722, 138–153. https://doi.org/10.1016/j.tecto.2017.10.016.
- Papanikolaou, D., Nomikou, P., Lampridou, D., 2018. Transverse tectonic zones delimiting seismic segments along prominent rift structures in the South Aegean: the Amorgos 1956 and Kos 2017 events. In: 9th International INQUA Meeting on Paleoseismology, Active Tectonics and Archeoseismology (PATA). Greece. Possidi, pp. 197–200, 25 –27 June 2018.
- Preine, J., and 32 others, 2025. Data report: core-seismic integration and time-depth relationships at IODP Expedition 398 Hellenic Arc Volcanic Field sites the Expedition 398 Scientists, Hellenic Arc Volcanic Field. In: Proceedings of the International Ocean Discovery Program, 398. https://doi.org/10.14379/iodp.proc.398.201.2025.
- Preine, J., Hübscher, C., Karstens, J., Nomikou, P., 2022a. Volcano-tectonic evolution of the Christiana-Santorini-Kolumbo Rift Zone. Tectonics 41, e2022TC007524. https:// doi.org/10.1029/2022TC007524.
- Preine, J., Karstens, J., Hübscher, C., Nomikou, P., Schmid, F., Crutchley, G.J., Druitt, T. H., Papanikolaou, D., 2022a. Spatio-temporal evolution of the Christiana-Santorini-Kolumbo volcanic field, Aegean Sea. Geology 50, 96–100. https://doi.org/10.1130/G49167.1.
- Rohling, E.J., Marino, G., Grant, K.M., 2015. Mediterranean climate and oceanography, and the periodic development of anoxic events (sapropels). Earth Sci. Rev. 143, 62–97. https://doi.org/10.1016/j.earscirev.2015.01.008.
- Rowland, J.V., Wilson, C.J., Gravley, D.M., 2010. Spatial and temporal variations in magma-assisted rifting, Taupo Volcanic Zone, New Zealand. J. Volcanol. Geotherm. Res. 190. 89–108. https://doi.org/10.1016/j.jvolgeores.2009.05.004.
- Sawyer, D.E., Urgeles, R., Iacono, C.L., 2023. 50,000 yr of recurrent volcaniclastic megabed deposition in the Marsili Basin, Tyrrhenian Sea. Geology 51, 1001–1006. https://doi.org/10.1130/G51198.1.
- Sparks, R.S.J., Annen, C., Blundy, J.D., Cashman, K.V., Rust, A.C., Jackson, M.D., 2019. Formation and dynamics of magma reservoirs. Phil. Trans. Roy. Soc. A 377, 20180019. https://doi.org/10.1098/rsta.2018.0019.
- Sternai, P., 2020. Surface processes forcing on extensional rock melting. Sci. Rep. 10, 7711. https://doi.org/10.1038/s41598-020-63920-w.
- Sternai, P., Jolivet, L., Menant, A., Gerya, T., 2014. Driving the upper plate surface deformation by slab rollback and mantle flow. Earth Planet. Sci. Lett. 405, 110–118. https://doi.org/10.1016/j.epsl.2014.08.023.
- Townsend, M., Huber, C., Degruyter, W., Bachmann, O., 2019. Magma chamber growth during intercaldera periods: insights from thermo-mechanical modeling with applications to Laguna del Maule, Campi Flegrei, Santorini, and Aso. Geochem. Geophys. Geosystems 20, 1574–1591. https://doi.org/10.1029/2018GC008103. Tsampouraki-Kraounaki, K., Sakellariou, D., Rousakis, G., Morfis, I., Panagiotopoulos, I.,
- Tsampouraki-Kraounaki, K., Sakellariou, D., Rousakis, G., Morfis, I., Panagiotopoulos, I., Livanos, I., Manta, K., Paraschos, F., Papatheodorou, G., 2021. The Santorini-Amorgos shear zone: evidence for dextral transtension in the South Aegean Back-Arc region, Greece. Geosci. (Basel) 11, 216. https://doi.org/10.3390/ geosciences11050216.
- Vougioukalakis, G.E., Satow, C.G., Druitt, T.H., 2019. Volcanism of the South Aegean volcanic arc. Elements 15, 159–164. https://doi.org/10.2138/gselements.15.3.159.
- Weinberg, R.F., Vernon, R.H., Schmeling, H., 2021. Processes in mushes and their role in the differentiation of granitic rocks. Earth Sci. Rev. 220, 103665.
- Wilson, C.J.N., Gravley, D.M., Leonard, G.S., Rowland, J.V., 2009. Volcanism in the Central Taupo Volcanic Zone, New Zealand: tempo, styles and controls. In: Thordarson, T., Self, S., Larsen, G., Rowland, S.K., Höskuldsson, Á. (Eds.), Studies in Volcanology: The Legacy of George Walker. Geol. Soc. Lond, pp. 225–248. https:// doi.org/10.1144/IAVCEI002.12.
- Wulf, S., Keller, J., Satow, C., Gertisser, R., Kraml, M., Grant, K.M., Appelt, O., Vakhrameeva, P., Koutsodendris, A., Hardiman, M., Schulz, H., Pross, J., 2020. Advancing Santorini's tephrostratigraphy: new glass geochemical data and improved marine-terrestrial tephra correlations for the past ~360 kyrs. Earth Sci. Rev. 200, 102964. https://doi.org/10.1016/j.earscirev.2019.102964.